

Large scale, selective dispersion of long single-walled carbon nanotubes with high photoluminescence quantum yield by shear force mixing



Arko Graf^a, Yuriy Zakharko^a, Stefan P. Schießl^a, Claudia Backes^a, Moritz Pfohl^{b, c}, Benjamin S. Flavel^b, Jana Zaumseil^{a, *}

^a Institute for Physical Chemistry, Universität Heidelberg, 69120 Heidelberg, Germany

^b Institute of Nanotechnology, Karlsruhe Institute of Technology, 76021 Karlsruhe, Germany

^c Institute of Materials Science, Technische Universität Darmstadt, 64287 Darmstadt, Germany

ARTICLE INFO

Article history:

Received 13 March 2016

Received in revised form

25 April 2016

Accepted 1 May 2016

Available online 2 May 2016

ABSTRACT

Selective dispersion of semiconducting single-walled carbon nanotube (SWCNTs) with conjugated polymers typically involves harsh sonication methods that damage and shorten the nanotubes. Here, we use simple high speed shear force mixing (SFM) to disperse nearly monochiral (6,5) SWCNTs with poly[(9,9-dioctylfluorenyl-2,7-diyl)-*alt-co*-(6,6'-{2,2'-bipyridine})] (PFO-BPy) in toluene with high yield and in large volumes. This highly scalable process disperses SWCNTs of exceptional quality with an average tube length of 1.82 μm and an ensemble photoluminescence quantum yield (PLQY) of 2.3%. For the first time for SWCNTs, we describe and apply absolute PLQY measurements, without the need for any reference emitter. We directly compare values for average SWCNT length, PLQY, linewidth and Stokes shift to other dispersion methods, including bath and tip sonication, as well as other sorting methods such as gel chromatography. We find that SFM results in dispersions of longer SWCNT with higher average PLQY than any other technique, thus making it an ideal method for sorting large amounts of long, high quality and purely semiconducting SWCNTs.

© 2016 The Authors. Published by Elsevier Ltd. This is an open access article under the CC BY-NC-ND license (<http://creativecommons.org/licenses/by-nc-nd/4.0/>).

1. Introduction

Semiconducting single-walled carbon nanotubes (SWCNTs) are one of the rare carbon-based materials that exhibit stable near-infrared (NIR) luminescence. In combination with their extremely high charge carrier mobilities and mechanical flexibility, SWCNTs could find applications in electronics [1,2], medicine [3], and optical telecommunication [4,5]. The spectral position of their very narrow emission line can be tuned across the entire NIR (900–2000 nm) by choosing the appropriate nanotube chirality (n,m), thus covering all optical telecommunication bands [6]. While for optoelectronic applications monochiral and purely semiconducting SWCNTs are necessary, SWCNT growth still yields mixtures of various semiconducting and metallic nanotube species [7]. Hence post-growth sorting is needed to supply SWCNTs as a pure and defined starting material. Importantly, this process has to be scalable beyond the

microgram-scale in order to become commercially viable. Among the various sorting techniques, such as gel chromatography [8], density gradient ultracentrifugation (DGU) [9], and aqueous two-phase separation [10], selectively wrapping SWCNTs with conjugated polymers leads to very pure semiconducting and even monochiral dispersions with comparatively low effort. For example, the polyfluorene copolymer poly[(9,9-dioctylfluorenyl-2,7-diyl)-*alt-co*-(6,6'-{2,2'-bipyridine})] (PFO-BPy, see Fig. 1a) yields almost monochiral (6,5) SWCNT dispersions [11–13]. In general, polymer-sorted SWCNTs exhibit very low residual metallic content and little intertube interactions, which results in the highest photoluminescence quantum yields (PLQY) in undoped ensemble samples reported so far [12,14,15].

Typically harsh sonication methods are used to disperse nanotubes in order to break up the SWCNT bundles of the raw material and enable surfactant or polymer wrapping [16,17]. Sonication of SWCNTs has two major problems. First, it is known to damage the carbon lattice and shorten the SWCNTs [15,18], due to high local pressure and friction forces that follow sonication-induced

* Corresponding author.

E-mail address: zaumseil@uni-heidelberg.de (J. Zaumseil).

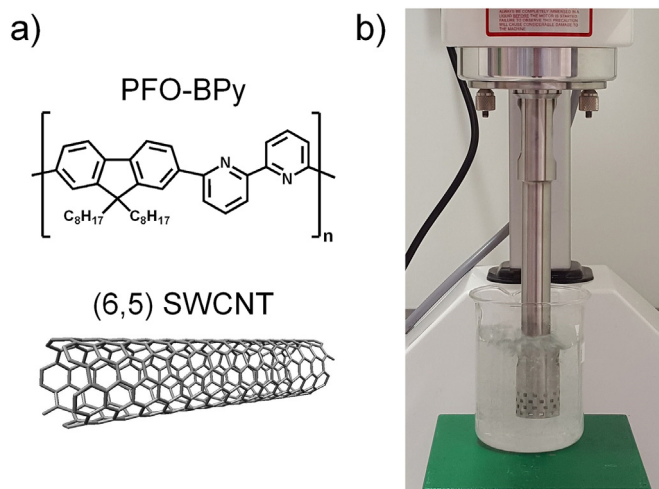


Fig. 1. (a) Molecular structure of copolymer PFO-BPy and (6,5) SWCNT. (b) Labscale shear force mixer used for dispersing large volumes of SWCNTs (cooling bath not shown). (A color version of this figure can be viewed online.)

cavitation. This is problematic because shorter nanotubes exhibit lower PLQY and, for example, in an SWCNT network field-effect transistor they necessitate more intertube charge transfers, which limits on-conductivity and effective mobility. Enrichment of the few remaining longer SWCNTs by size-exclusion chromatography, zonal fractionation or precipitation is time consuming and limited in maximum length ($\sim 1 \mu\text{m}$) and concentration [19–21]. Second, sonication suffers from reproducibility issues and its scalability to industrially relevant quantities has not yet been shown. Other methods for the dispersion of SWCNTs include turbulent flow and mechanical force with (e.g. ball mill) or without (e.g. shear force mixer) grinding media [22]. Recently these dispersion methods have been investigated with regard to layered materials such as graphene [23] or MoS_2 [24]. The application of shear forces, for example by high speed shear force mixing (SFM) was found to be highly efficient as well as less damaging than sonication. Further, the scalability of SFM up to hundreds of liters was shown for liquid graphene exfoliation and is a well-understood industrial process for emulsions [25]. Despite its simplicity and low cost, SFM has not yet been applied for selective polymer dispersion of SWCNTs and only very rarely for the dispersion of SWCNTs in aqueous surfactant solutions [26]. This may be due to the misconception that it only yields small amounts of SWCNTs.

Here, we demonstrate that high speed SFM is suitable for large-volume, high-yield, high-quality and highly selective dispersion of carbon nanotubes by polymer wrapping using (6,5) SWCNTs as an example system. In particular, SFM yields large amounts of exceptionally long SWCNTs. These SWCNTs exhibit a considerably higher PLQY than previously reported ensemble averages, thus confirming the high quality of the shear force dispersed SWCNTs. Furthermore, for the first time for SWCNTs, the absolute PLQYs were measured directly and without any reference emitter for low and high concentrations. We compare these PLQY values with those of SWCNTs dispersed by different sonication methods and confirm the superior properties of shear-force mixed SWCNT dispersions.

2. Experimental

2.1. SWCNT dispersion and recycling

All (6,5) SWCNT dispersions were prepared from the same CoMoCAT[®] raw material (Sigma Aldrich 773735, Lot #14J017A1).

According to the supplier, this CoMoCAT material has a maximum carbon content of 95%, of which 93% are SWCNTs. 40% of the nanotubes are (6,5) SWCNTs resulting in a total of $\sim 35 \text{ wt\%}$ of the raw material. For polymer-wrapping with SFM, 0.5 g/L PFO-BPy (American Dye Source, $M_w = 34 \text{ kg/mol}$) were dissolved in 140 mL toluene before adding 0.38 g/L CoMoCAT raw material. Hence, a maximum of 17 mg (6,5) SWCNTs was in the initial dispersion. SFM using a Silverson L5M-A mixer was then applied at maximum speed (10,230 rpm) for a given time. The temperature was kept constant at 20°C with a cooling bath. The dispersion step was followed by centrifugation at 60,000 g (Beckman Coulter Avanti J26XP centrifuge) for 45 min with an intermediate supernatant extraction and centrifuge tube exchange after 15 min. For SWCNT recycling the pellet obtained after centrifugation and supernatant extraction was reused instead of raw CoMoCAT material. Fresh toluene (140 mL) and polymer (0.5 g/L) were added to the pelletized nanotubes and SFM was repeated.

For comparison, 10 mL (20 mL) of toluene with 2 g/L (0.5 g/L) PFO-BPy and 1.5 g/L (0.38 g/L) CoMoCAT were used for dispersions employing bath (tip) sonication for 6 h (5.5 h). During the treatment with the ultrasonic bath (Bandelin Sonorex Digitec DT 102 H) or the tip sonicator (Sonics Vibra Cell, pulsed mode at 20% power output) the temperature was kept constant at 20°C . Again, the dispersion step was followed by centrifugation at 60,000 g for 45 min with an intermediate supernatant extraction and centrifuge tube exchange after 15 min.

Surfactant suspended (6,5) SWCNTs were prepared from the same CoMoCAT material similar to previous work [17]. Briefly, 15 mg raw material was suspended in 2 wt% aqueous sodium dodecyl sulfate (SDS, Merck) solution by tip sonication (Weber Ultrasonics, 35 kHz, 500 W, in continuous mode at $\sim 20\%$ power output) for 1 h at 15°C . After sonication, the suspension was centrifuged at 100,000 g for 1 h and carefully decanted. Due to the high affinity of (6,5) to the Sephacryl-S200 gel (Amersham Biosciences) at 1.6 wt% SDS the concentration was adjusted by addition of water before being applied to a gel column in a one-column approach. 1 wt% sodium cholate (Sigma Aldrich) was used as the eluent. DGU was performed in a 1 wt% sodium cholate solution with a stepped density gradient of Iodixanol (from bottom to top of the centrifuge tube) 40 wt%/30 wt% + (6,5) SWCNTs/20 wt%.

2.2. Length measurements

The length distribution of the dispersed SWCNTs was determined by recording tapping-mode atomic force microscopy (AFM) images (Bruker Dimension Icon) of well-separated SWCNTs on a polished silicon wafer. Dispersions were directly spin-coated onto the wafer and residual polymer or surfactant was washed off with THF. The lengths of more than 200 nanotubes per sample were analyzed.

2.3. Optical characterization

Absorption spectra were recorded with a Varian Cary 6000i spectrometer with an optical path length of 10 mm. For photoluminescence excitation-emission (PLE) maps of the SWCNT dispersion the spectrally separated output of a WhiteLase SC400 supercontinuum laser source (Fianium Ltd.) was used for excitation and spectra were recorded with an Acton SpectraPro SP2358 (grating 150 lines/mm) spectrometer with an OMA-V InGaAs line camera (Princeton Instruments) and corrected for background and wavelength-dependent sensitivity/excitation power.

2.4. Direct PLQY measurement

The photoluminescence quantum yield (PLQY), was directly determined by measuring the ratio of emitted to absorbed photons as introduced by de Mello et al. [27]. Briefly, in a first measurement a cuvette containing the solvent was placed within the integrating sphere (LabSphere, Spectralon Coating) and the intensity of the excitation laser (575 nm) was recorded. Then the dispersion of (6,5) SWCNTs was inserted and both the emission spectra and the attenuated laser peak were recorded. The integrated difference of the laser intensity correlates with the number of absorbed photons. Similarly the integral over the emission spectra correlates with the number of emitted photons. Taking the ratio of those quantities directly gives the PLQY. For high concentration samples a self-absorption correction was applied according to Ahn et al. [28].

For excitation we used a 1 nm wide part around 575 nm (resonant with the E_{22} transition of (6,5) SWCNTs) of a WhiteLase SC400 supercontinuum laser (Fianium Ltd.). The output power was monitored during the measurement and fluctuations were accounted for in the analysis. Emission signals from the sphere were transmitted via an optical fiber and coupled into Acton SpectraPro SP2358 (grating 150 lines/mm) spectrometer with an OMA-V InGaAs line camera (Princeton Instruments) for spectra acquisition. Careful correction of the wavelength-dependent transmissivity of all optical components as well as detector sensitivity were taken into account. For a more detailed description, including a representative data set see [Supplementary Information Section S1](#).

3. Results and discussion

3.1. Dispersion and length distribution

A commercial lab-scale high speed shear force mixer (Silverson L5M-A, Fig. 1b) with a precisely fitted rotor in a workhead (stator) with small perforations was employed for the dispersion of nanotubes in polymer solution. During mixing, the fast rotation of the rotor pulls in material from underneath. The material is then milled within the workhead and spun out under high shear forces. For selective dispersion of (6,5) nanotubes, a PFO-BPy/CoMoCAT/toluene suspension was mixed for up to 92 h. Note that during mixing no supervision or other work was required. After centrifugation, the final supernatant (>120 mL) was purple, which already indicated the high concentration of nanotubes due to the E_{22} absorption at 575 nm of (6,5) SWCNTs. The high nanotube concentration was confirmed by the absorption spectrum of the dispersion (Fig. 2a, black line) with an absorbance at E_{11} exceeding 1.3 cm^{-1} (absorbance normalized to length of light path). In addition to the two main absorption peaks (E_{11} and E_{22}) of (6,5) SWCNTs a phonon sideband at 857 nm and 526 nm can be observed for both transitions, respectively [29–31]. Within the detection limit no metallic nanotubes were found.

For evaluation of the distribution of semiconducting chiralities within the dispersion we recorded PLE maps (see [Supplementary Information Fig. S2](#)). Almost negligible emission from (9,5), (7,5), (8,3) and (9,1) SWCNTs was detected in addition to the dominant (6,5) emission at 997.7 nm (see [Supplementary Information Fig. S3a](#)). We estimated the relative chirality distribution from the absorption spectrum by applying a multi-peak fitting routine ([Supplementary Information Fig. S3b and Table S1](#)). Assuming nearly chirality-independent molar absorptivity [32], a (6,5) SWCNT content of more than 84% was found.

The high purity was reached by removing insufficiently debundled SWCNTs by centrifugation, which in turn results in the loss of a significant portion of the raw material. However, this

material can be recycled and subjected to further shear force mixing by adding fresh polymer solution using the same toluene volume and polymer concentration. Surprisingly, recycling with another SFM step for 48 h and subsequent centrifugation led to an even higher (~3 times) SWCNT concentration, as shown in the absorption spectrum in Fig. 2a (purple line). The supernatant had a deep purple color, shown in Fig. 2b. By recycling the material three times we extracted 1.8 mg of (6,5) SWCNTs in total, which is more than 10% of the approximately 17 mg of (6,5) SWCNTs in the raw material (see Fig. 2a and [Supplementary Information Fig. S4](#)) and could possibly be increased further by more recycling rounds. A similar multiple extraction process was previously used for large diameter SWCNTs and dispersion by sonication [33] and could be a general method to enhance overall yields.

While recycling is important to minimize material wastage, we will focus here on the properties of the (6,5) SWCNTs selected directly after the first SFM dispersion step. To determine the time (t) dependence of the SWCNT dispersion yield by SFM, we recorded the (6,5) SWCNT concentration (E_{11} absorbance per cm path length) of 2 mL samples that were successively taken from the main solution during shear mixing (Fig. 2c). Initially, the amount of dispersed (6,5) SWCNTs increased quickly but then saturated. The data can be fitted with a power law of $t^{0.66}$. Interestingly, this trend is equal to that for shear force mixed graphene, albeit on a much longer timescale [23]. Alternatively, the (6,5) SWCNT concentration $c(t)$ (proportional to the absorbance) can be fitted by a saturation model

$$c(t) = c_{\max} \frac{t}{t_{1/2} + t} \quad (1)$$

where c_{\max} is the maximum concentration and $t_{1/2}$ is the time after which $0.5 \cdot c_{\max}$ is reached. The fit gives a maximum E_{11} absorbance of 1.9 cm^{-1} (i.e., 3.3 mg/L) with $t_{1/2} = 38 \text{ h}$ (solid line in Fig. 2c). The SWCNT concentration (as carbon mass) was calculated by using a molar peak absorptivity of $6700 \text{ M}^{-1} \text{ cm}^{-1}$ [32].

As shown above, the absolute yield of dispersed SWCNTs after almost 4 days of SFM is already very high, but such long processing times could also damage and shorten the nanotubes. Hence, the length of the sorted (6,5) SWCNTs after 92 h of SFM was determined by AFM measurements. The dispersion was spin-coated on a polished Si wafer and rinsed with THF to remove residual polymer. The length of 340 individual SWCNTs dispersed by SFM was evaluated (see [Supplementary Information Fig. S5](#)). Fig. 3 shows the length distribution with an average SWCNT length of $1.82 \mu\text{m}$ (standard deviation $1.12 \mu\text{m}$, median length $1.55 \mu\text{m}$) and a good proportion (>40%) of nanotubes longer than $2 \mu\text{m}$. The long average length suggests that damage and scission during SFM are minimal. These SWCNTs are much longer than nanotubes dispersed by any technique that involves sonication [15,17,26]. Reference samples obtained by bath and tip sonication showed substantially shorter nanotubes (see Fig. 3 and [Supplementary Information Table S2](#)). Note that by using shear force mixing at lower speeds and for shorter times the average length could possibly be increased even further similar to the size of graphene flakes dispersed by SFM [23]. In addition to advances for electronic applications such as field-effect transistors [34], long SWCNTs should exhibit higher PLQYs in dispersion [12]. Very bright emission was previously shown for air-suspended SWCNTs with length of tens of micrometers [35].

3.2. Direct PLQY measurement

The PLQY of the SWCNTs will strongly influence any photonic and optoelectronic application and thus needs to be carefully evaluated. Being defined as the ratio of emitted to absorbed

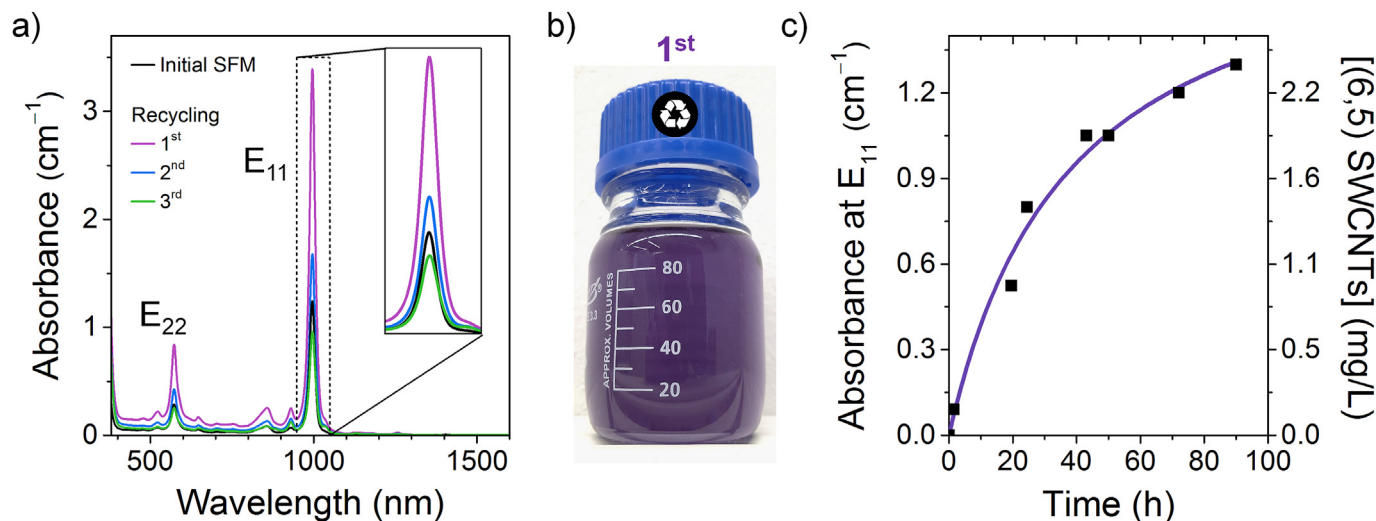


Fig. 2. (a) Absorption spectrum of (6,5) SWCNTs wrapped with PFO-BPy after 92 h of SFM and subsequent centrifugation (black line) exhibiting an absorbance at E₁₁ of (6,5) SWCNTs exceeding 1.3 cm⁻¹. Recycling of unwrapped material strongly increases the SWCNT concentration in the first round (purple line, 1st) and disperses additional nanotubes when repeated (2nd and 3rd recycling round, blue and green line). (b) Photograph of 100 ml of purple supernatant of recycled (6,5) SWCNTs (1st round). (c) Time dependence of the absorbance at E₁₁ and corresponding carbon concentration for (6,5) SWCNTs during SFM. (A color version of this figure can be viewed online.)

photons, the PLQY is at the same time an unambiguous measure of the SWCNT quality. Small amounts of non-radiative defects, including disruptions in the carbon lattice and open ends of an

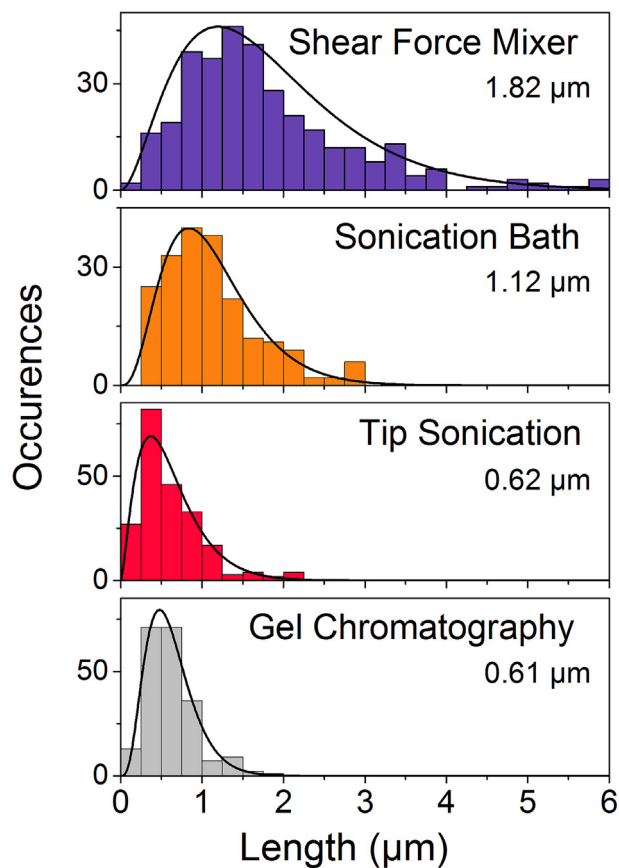


Fig. 3. Length distribution as determined by AFM of sorted (6,5) SWCNTs using different dispersion methods with their mean length. SWCNTs dispersed by 92 h of SFM clearly lead to the longest tubes with a mean length of 1.82 μm. (A color version of this figure can be viewed online.)

SWCNT, as well as residual metallic SWCNTs and catalyst particles increase loss channels and thus lead to a drastically reduced PLQY [26,36]. However, it has been difficult to determine the absolute PLQY values for SWCNT ensembles due to the problem of polydispersity, absorption background, low concentrations and simultaneous detection in the visible (excitation) and NIR (emission). Hence, relative methods are often applied using a reference emitter, usually the NIR dye Styryl 13 [27,28]. Unfortunately, the PLQY values of this emitter vary from batch to batch and depend on the freshness of the material/dispersions and the way the dye was dispersed (sonication etc.) [37]. Careful studies determined the PLQY of Styryl 13 to be between 2.0% and 3.5% [12,37]. Due to this spread of PLQY values the use of Styryl 13 in relative measurements introduces uncertainties for the final PLQY values of more than 40%. Moreover, some SWCNT studies incorrectly used a PLQY for Styryl 13 of 11% [38,39], which led to an overestimation of the final SWCNT PLQY by a factor of 3–5. Absolute techniques for the determination of the PLQY are thus clearly necessary to obtain dependable reference values.

Here, we applied an absolute measurement of the PLQY by simultaneously recording absorption and emission spectra in a calibrated integrating sphere avoiding the need for any reference emitter as introduced by de Mello et al. [27] and usually applied for emitters in the visible spectrum. For a detailed description of the measurement and setup the reader is referred to the experimental section and [Supplementary Information Section S1](#).

We emphasize that for these measurements, in contrast to the majority of SWCNT photoluminescence studies, no reference emitter was needed. Moreover, we excluded any influence of scattering, which typically introduces more uncertainties due to the need of background correction [40]. To verify our measurement technique, we also measured the PLQY of Styryl 13. For a fresh dispersion in methanol obtained by mild bath sonication for 5 min we found a PLQY of (3.5 ± 0.2) % for concentrations between 0.01 and 1 g/L, which is in good agreement with the literature [12,37].

SWCNTs dispersed by 43 h of SFM exhibited an average PLQY of 2.4% for (6,5) concentrations between 0.1 and 1.4 mg/L (see Fig. 4). In comparison, for SWCNTs being mixed for 92 h, that is, more than twice as long, we found an average PLQY of 2.3%, which is essentially identical to the former within the precision of the

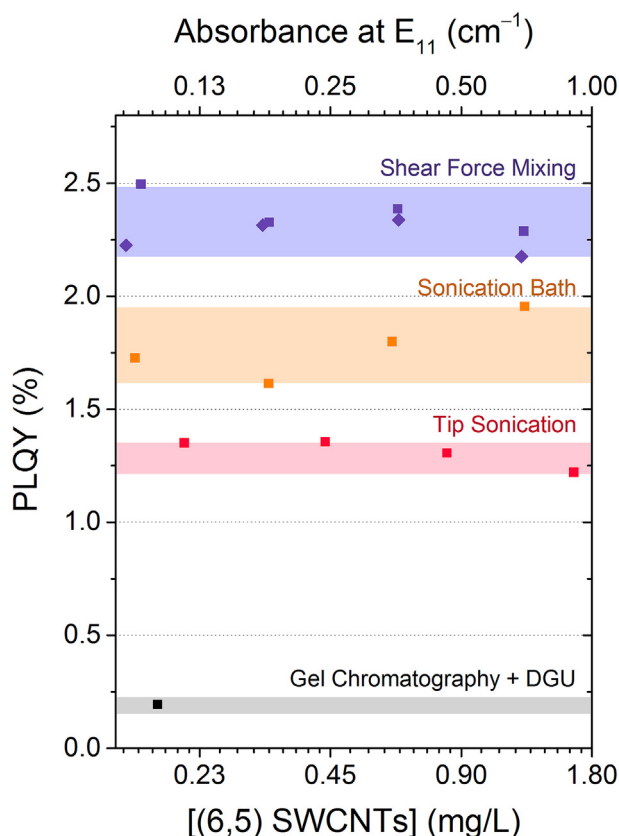


Fig. 4. PLQY values of (6,5) SWCNTs dispersed by SFM (purple) for 43 h (squares) and 92 h (diamonds) at different concentrations. SWCNT concentrations were varied by adding pure solvent to the dispersion. The PLQY for (6,5) SWCNTs dispersed by bath sonication (orange), tip sonication (pink) and dispersion in water with SDS followed by gel chromatography and density gradient centrifugation (gray) are shown for comparison. (A color version of this figure can be viewed online.)

measurement. The almost unchanged PLQY for longer mixing times corroborates the low impact of SFM on the structure of the SWCNTs. In addition, there is no significant roll-off of the PLQY at high concentrations for both samples confirming good SWCNT individualization and negligible amounts of metallic SWCNTs in the dispersion.

To further benchmark the quality of the SWCNTs dispersed by SFM, we compared them to SWCNTs dispersed by sonication. For direct comparison we started with the same CoMoCAT raw material and polymer solution but using bath sonication (SB) or a tip sonicator (sonic disintegrator, SD) for moderate sonication times (see [Experimental](#)). The (6,5) SWCNTs dispersed by bath sonication exhibited a PLQY of 1.8% and the stronger tip sonication led to a PLQY of 1.3% (see [Fig. 4](#)), which is significantly below the values for

shear force mixed samples (PLQY = 2.3%), while the purity of these dispersions is similar ([Supplementary Information Table S1](#)). In addition, we prepared (6,5) SWCNTs suspended in aqueous sodium dodecyl sulfate (SDS) solution and purified by gel chromatography, which also involves tip sonication for dispersion, and an additional density gradient ultracentrifugation (DGU) step (see [Experimental](#)). The PLQY of these (6,5) SWCNTs was measured to be only 0.2%. Note that the purity of these samples might be further increased by repetitive DGU, however, the PLQY would most likely not exceed 1% [12].

As shown in [Fig. 3](#) and summarized in [Table 1](#) SFM yields longer nanotubes than sonication methods. Clearly, SWCNT scission occurs when the nanotubes are sonicated even for moderate times (few hours) and the shortest nanotubes (average length 0.6 μm) are found when strong tip sonication is used. In agreement with previous reports, nanotube ensembles with longer SWCNTs exhibit higher average PLQY values due to the lower probability of quenching at the nanotube ends [12,15,26]. Owing to the forces that lead to SWCNT scission, it is likely that shorter nanotubes also have more defects in the carbon lattice per unit length [26]. The high PLQY of (6,5) SWCNTs dispersed by SFM confirms that SFM is a mild dispersion method that yields long and high-quality SWCNTs without the need for any further purification or length fractionation. Not only the quality but also the yield of polymer-wrapped nanotubes is significantly higher with SFM than for dispersion by sonication (see [Table 1](#)). In direct comparison to SWCNTs dispersed by tip sonication, SFM is twice as efficient as well as more reproducible.

Careful assessment of the PL and absorption peaks ([Fig. 5](#)) of the different polymer-wrapped (6,5) SWCNTs further supports the notion of different defect densities. Stronger sonication leads to a red-shift and broadening of the absorption as well as the emission peaks (see [Table 1](#)). The red-shift, however, is stronger for emission than for absorption leading to an increased Stokes shift (from 2.2 to 3.2 meV) for harsher dispersion conditions. We attribute this increased Stokes shift to defect-induced mid-gap states [41]. While the absorption is always dominated by the pristine part of the SWCNT and thus shifts only slightly, the highly mobile excitons will find trap sites and thus lead to a stronger shift of the emission. The full width at half maximum (FWHM) of the E_{11} and E_{22} absorption peaks and the E_{11} emission peak also increase from SFM to tip sonication ([Supplementary Information Fig. S6](#)). Moreover, additional Raman spectroscopy ([Supplementary Information Fig. S7 and Tables S3 and S4](#)) of the dispersed SWCNTs reveals a larger $G^+/2D$ peak area ratio for stronger sonication, which was previously shown to inversely correlate with the PLQY and might be a useful and independent measure for the SWCNT quality [36].

The direct comparison to (6,5) SWCNTs dispersed in aqueous SDS solution is less clear as the surfactant and solvent lead to a substantial shift and broadening of the emission and absorption peaks. The low PLQY might be an effect of residual metallic SWCNTs

Table 1

Summary of optical properties and average lengths of (6,5) SWCNTs dispersed with different techniques.

	SFM (92 h)	Bath sonication (6 h)	Tip sonication (5.5 h)	SDS (DGU)
PLQY (%)	2.3	1.8	1.3	0.2
Mean length (μm)	1.82	1.12	0.61	0.62
λ_{ABS} (nm) (E_{11})	996.1	996.3	996.3	1001.6
λ_{EM} (nm)	997.7	998.2	999.6	1006.7
Stokes shift (meV)	2.2	2.5	3.2	5.2
E_{22} FWHM _{ABS} (meV)	54.3	55.2	56.6	102.1
E_{11} FWHM _{ABS} (meV)	20.1	21.1	22.4	49.4
E_{11} FWHM _{EM} (meV)	23.1	24.6	27.7	51.1
(6,5)-Yield (%)	1.67	0.07	0.82	–

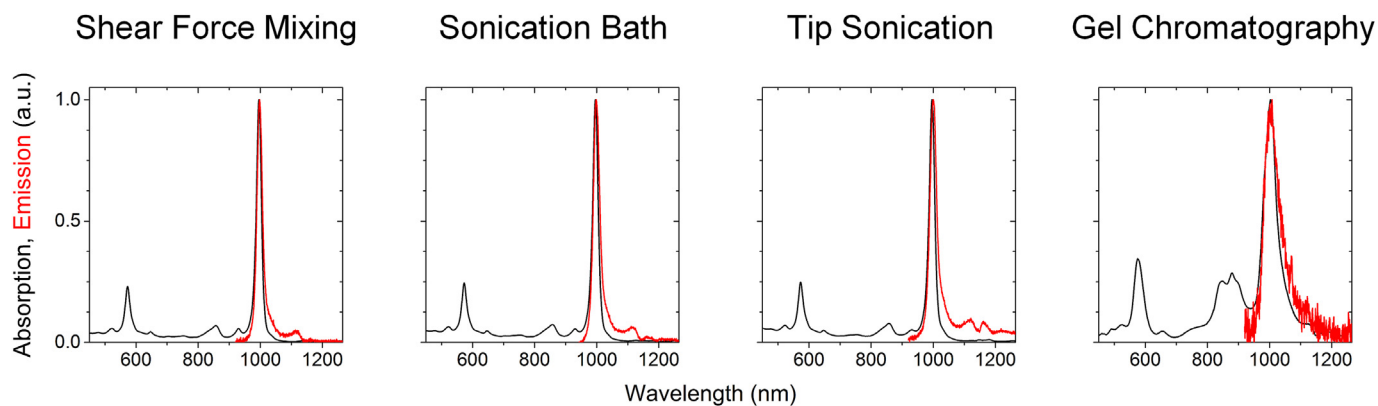


Fig. 5. Normalized absorbance and PL spectra (excited at 575 nm) of all dispersions. These spectra were used to determine the peak positions and widths of the E_{11} transition for absorption and emission. Note, the absorbance for the gel chromatography samples was background-corrected. (A color version of this figure can be viewed online.)

and lower surfactant coverage, which may allow access of quenchers (e.g. O_2) to the SWCNT surface.

In summary, we showed that shear force mixing is a scalable, reproducible and efficient method for the dispersion of SWCNTs with conjugated polymers that yields high-quality, nearly monochiral dispersions of exceptionally long (6,5) nanotubes with high photoluminescence efficiencies. With this simple method the cost of sorting SWCNTs could be significantly reduced while improving the material quality at the same time. The obtained long SWCNTs are ideal for optoelectronic applications, for which large amounts of high purity semiconducting SWCNTs are required.

Acknowledgments

This research was financially supported by the European Research Council under the European Union's Seventh Framework Programme (FP/2007–2013)/ERC Grant Agreement No. 306298 (EN-LUMINATE). J.Z. and C.B. thank the Alfred Krupp von Bohlen und Halbach-Stiftung for general support. B.S.F. gratefully acknowledges support from the Deutsche Forschungsgemeinschaft's Emmy Noether Program under grant number FL 834/1-1. We acknowledge Tobias Schenk for help with initial SFM experiments.

Appendix A. Supplementary data

Supplementary data related to this article can be found at <http://dx.doi.org/10.1016/j.carbon.2016.05.002>.

References

- [1] S.P. Schiefl, N. Fröhlich, M. Held, F. Gannott, M. Schweiger, M. Forster, et al., Polymer-sorted semiconducting carbon nanotube networks for high-performance ambipolar field-effect transistors, *ACS Appl. Mater. Interfaces* 7 (2015) 682–689, <http://dx.doi.org/10.1021/am506971b>.
- [2] M.L. Geier, J.J. McMorrow, W. Xu, J. Zhu, C.H. Kim, T.J. Marks, et al., Solution-processed carbon nanotube thin-film complementary static random access memory, *Nat. Nanotechnol.* 10 (2015) 944–948, <http://dx.doi.org/10.1038/nnano.2015.197>.
- [3] N.M. Iverson, P.W. Barone, M. Shandell, L.J. Trudel, S. Sen, F. Sen, et al., In vivo biosensing via tissue-localizable near-infrared-fluorescent single-walled carbon nanotubes, *Nat. Nanotechnol.* 8 (2013) 873–880, <http://dx.doi.org/10.1038/nnano.2013.222>.
- [4] S. Khasminkaya, F. Pyatkov, B.S. Flavel, W.H. Pernice, R. Krupke, Waveguide-integrated light-emitting carbon nanotubes, *Adv. Mater.* 26 (2014) 3465–3472, <http://dx.doi.org/10.1002/adma.201305634>.
- [5] F. Jakubka, C. Backes, F. Gannott, U. Mundloch, F. Hauke, A. Hirsch, et al., Mapping charge transport by electroluminescence in chirality-selected carbon nanotube networks, *ACS Nano* 7 (2013) 7428–7435, <http://dx.doi.org/10.1021/nn403419d>.
- [6] S.M. Bachilo, M.S. Strano, C. Kittrell, R.H. Hauge, R.E. Smalley, R.B. Weisman, Structure-assigned optical spectra of single-walled carbon nanotubes, *Science* 298 (2002) 2361–2366, <http://dx.doi.org/10.1126/science.1078727>.
- [7] M. Schweiger, M. Schaudig, F. Gannott, M.S. Killian, E. Bitzek, P. Schmuki, et al., Controlling the diameter of aligned single-walled carbon nanotubes on quartz via catalyst reduction time, *Carbon N. Y.* 95 (2015) 452–459, <http://dx.doi.org/10.1016/j.carbon.2015.08.058>.
- [8] H. Liu, D. Nishide, T. Tanaka, H. Kataura, Large-scale single-chirality separation of single-wall carbon nanotubes by simple gel chromatography, *Nat. Commun.* 2 (2011) 309, <http://dx.doi.org/10.1038/ncomms1313>.
- [9] S. Ghosh, S.M. Bachilo, R.B. Weisman, Advanced sorting of single-walled carbon nanotubes by nonlinear density-gradient ultracentrifugation, *Nat. Nanotechnol.* 5 (2010) 443–450, <http://dx.doi.org/10.1038/nnano.2010.68>.
- [10] K.E. Moore, D.D. Tune, B.S. Flavel, Double-walled carbon nanotube processing, *Adv. Mater.* 27 (2015) 3105–3137, <http://dx.doi.org/10.1002/adma.201405686>.
- [11] W. Gomulya, J. Gao, M.A. Loib, Conjugated polymer-wrapped carbon nanotubes: physical properties and device applications, *Eur. Phys. J. B* 86 (2013) 404, <http://dx.doi.org/10.1140/epjb/e2013-40707-9>.
- [12] T. Hertel, S. Himmelein, T. Ackermann, D. Stich, J. Crochet, Diffusion limited photoluminescence quantum yields in 1-D semiconductors: single-wall carbon nanotubes, *ACS Nano* 4 (2010) 7161–7168, <http://dx.doi.org/10.1021/nn101612b>.
- [13] H. Ozawa, N. Ide, T. Fujigaya, Y. Niidome, N. Nakashima, One-pot separation of highly enriched (6,5)-single-walled carbon nanotubes using a fluorene-based copolymer, *Chem. Lett.* 40 (2011) 239–241, <http://dx.doi.org/10.1246/cl.2011.239>.
- [14] A. Nish, J.-Y. Hwang, J. Doig, R.J. Nicholas, Highly selective dispersion of single-walled carbon nanotubes using aromatic polymers, *Nat. Nanotechnol.* 2 (2007) 640–646, <http://dx.doi.org/10.1038/nnano.2007.290>.
- [15] S. Mouri, Y. Miyauchi, K. Matsuda, Dispersion-process effects on the photoluminescence quantum yields of single-walled carbon nanotubes dispersed using aromatic polymers, *J. Phys. Chem. C* 116 (2012) 10282–10286, <http://dx.doi.org/10.1021/jp212040y>.
- [16] F. Bottacchi, L. Petti, F. Späth, I. Namal, G. Tröster, T. Hertel, et al., Polymer-sorted (6,5) single-walled carbon nanotubes for solution-processed low-voltage flexible microelectronics, *Appl. Phys. Lett.* 106 (2015) 193302–193304, <http://dx.doi.org/10.1063/1.4921078>.
- [17] B.S. Flavel, K.E. Moore, M. Pfohl, M.M. Kappes, F. Hennrich, Separation of single-walled carbon nanotubes with a gel permeation chromatography system, *ACS Nano* 8 (2014) 1817–1826, <http://dx.doi.org/10.1021/nn4062116>.
- [18] F. Hennrich, R. Krupke, K. Arnold, J.A. Rojas Stütz, S. Lebedkin, T. Koch, et al., The mechanism of cavitation-induced scission of single-walled carbon nanotubes, *J. Phys. Chem. B* 111 (2007) 1932–1937, <http://dx.doi.org/10.1021/jp065262n>.
- [19] H. Gui, H. Chen, C.Y. Khripin, B. Liu, J.A. Fagan, C. Zhou, et al., A facile and low-cost length sorting of single-wall carbon nanotubes by precipitation and applications for thin-film transistors, *Nanoscale* 8 (2016) 3467–3473, <http://dx.doi.org/10.1039/C5NR07329D>.
- [20] C.Y. Khripin, X. Tu, J.M. Heddleston, C. Silvera-Batista, A.R. Hight Walker, J. Fagan, et al., High-resolution length fractionation of surfactant-dispersed carbon nanotubes, *Anal. Chem.* 85 (2013) 1382–1388, <http://dx.doi.org/10.1021/acs303349q>.
- [21] F. Hennrich, W. Li, R. Fischer, S. Lebedkin, R. Krupke, M.M. Kappes, Length-sorted, large-diameter, polyfluorene-wrapped semiconducting single-walled carbon nanotubes for high-density, short-channel transistors, *ACS Nano* 10 (2016) 1888–1895, <http://dx.doi.org/10.1021/acsnano.5b05572>.
- [22] H. Yoon, M. Yamashita, S. Ata, D.N. Futaba, T. Yamada, K. Hata, Controlling exfoliation in order to minimize damage during dispersion of long SWCNTs for advanced composites, *Sci. Rep.* 4 (2014) 3907, <http://dx.doi.org/10.1038/srep03907>.
- [23] K.R. Paton, E. Varrla, C. Backes, R.J. Smith, U. Khan, A. O'Neill, et al., Scalable

- production of large quantities of defect-free few-layer graphene by shear exfoliation in liquids, *Nat. Mater* 13 (2014) 624–630, <http://dx.doi.org/10.1038/nmat3944>.
- [24] E. Varrla, C. Backes, K.R. Paton, A. Harvey, Z. Gholamvand, J. McCauley, et al., Large-scale production of size-controlled MoS₂ nanosheets by shear exfoliation, *Chem. Mater* 27 (2015) 1129–1139, <http://dx.doi.org/10.1021/cm5044864>.
- [25] S. Hall, M. Cooke, A.W. Pacey, A.J. Kowalski, D. Rothman, Scaling up of silverson rotor-stator mixers, *Can. J. Chem. Eng.* 89 (2011) 1040–1050, <http://dx.doi.org/10.1002/cjce.20556>.
- [26] A.V. Naumov, D.A. Tsybolski, S.M. Bachilo, R.B. Weisman, Length-dependent optical properties of single-walled carbon nanotube samples, *Chem. Phys.* 422 (2013) 255–263, <http://dx.doi.org/10.1016/j.chemphys.2012.12.033>.
- [27] J.C. de Mello, H.F. Wittmann, R.H. Friend, An improved experimental determination of external photoluminescence quantum efficiency, *Adv. Mater* 9 (1997) 230–232, <http://dx.doi.org/10.1002/adma.19970090308>.
- [28] T.-S. Ahn, R.O. Al-Kaysi, A.M. Müller, K.M. Wentz, C.J. Bardeen, Self-absorption correction for solid-state photoluminescence quantum yields obtained from integrating sphere measurements, *Rev. Sci. Instrum.* 78 (2007) 086105, <http://dx.doi.org/10.1063/1.2768926>.
- [29] M.S. Arnold, J.L. Blackburn, J.J. Crochet, S.K. Doorn, J.G. Duque, A. Mohite, et al., Recent developments in the photophysics of single-walled carbon nanotubes for their use as active and passive material elements in thin film photovoltaics, *Phys. Chem. Chem. Phys.* 15 (2013) 14896–14918, <http://dx.doi.org/10.1039/c3cp52752b>.
- [30] Y. Miyauchi, Photoluminescence studies on exciton photophysics in carbon nanotubes, *J. Mater. Chem. C* 1 (2013) 6499–6521, <http://dx.doi.org/10.1039/c3tc00947e>.
- [31] J.L. Blackburn, J.M. Holt, V.M. Irurzun, D.E. Resasco, G. Rumbles, Confirmation of K-Momentum dark exciton vibronic sidebands Using ¹³C-labeled, highly enriched (6,5) single-walled carbon nanotubes, *Nano Lett.* 12 (2012) 1398–1403, <http://dx.doi.org/10.1021/nl204072x>.
- [32] J.K. Streit, S.M. Bachilo, S. Ghosh, C.-W. Lin, R.B. Weisman, Directly measured optical absorption cross sections for structure-selected single-walled carbon nanotubes, *Nano Lett.* 14 (2014) 1530–1536, <http://dx.doi.org/10.1021/nl404791y>.
- [33] J. Ding, Z. Li, J. Lefebvre, F. Cheng, G. Dubey, S. Zou, et al., Enrichment of large-diameter semiconducting SWCNTs by polyfluorene extraction for high network density thin film transistors, *Nanoscale* 6 (2014) 2328–2339, <http://dx.doi.org/10.1039/c3nr05511f>.
- [34] Y. Miyata, K. Shiozawa, Y. Asada, Y. Ohno, R. Kitaura, T. Mizutani, et al., Length-sorted semiconducting carbon nanotubes for high-mobility thin film transistors, *Nano Res.* 4 (2011) 963–970, <http://dx.doi.org/10.1007/s12274-011-0152-7>.
- [35] J. Lefebvre, D.G. Austing, J. Bond, P. Finnie, Photoluminescence imaging of suspended single-walled carbon nanotubes, *Nano Lett.* 6 (2006) 1603–1608, <http://dx.doi.org/10.1021/nl060530e>.
- [36] M. Kastner, S. Stahl, I. Vollert, C. Loi, N. Rühl, T. Hertel, et al., A comparison of Raman and photoluminescence spectra for the assessment of single-wall carbon nanotube sample quality, *Chem. Phys. Lett.* 635 (2015) 245–249, <http://dx.doi.org/10.1016/j.cplett.2015.06.076>.
- [37] N. Stürzl, S. Lebedkin, M.M. Kappes, Revisiting the laser dye styryl-13 as a reference near-infrared fluorophore: implications for the photoluminescence quantum yields of semiconducting single-walled carbon nanotubes, *J. Phys. Chem. A* 113 (2009) 10238–10240, <http://dx.doi.org/10.1021/jp905166s>.
- [38] J. Crochet, M. Clemens, T. Hertel, Quantum yield heterogeneities of aqueous single-wall carbon nanotube suspensions, *J. Am. Chem. Soc.* 129 (2007) 8058–8059, <http://dx.doi.org/10.1021/ja071553d>.
- [39] Y. Piao, B. Meany, L.R. Powell, N. Valley, H. Kwon, G.C. Schatz, et al., Brightening of carbon nanotube photoluminescence through the incorporation of sp³ defects, *Nat. Chem.* 5 (2013) 840–845, <http://dx.doi.org/10.1038/nchem.1711>.
- [40] S.-Y. Ju, W.P. Kopcha, F. Papadimitrakopoulos, Brightly fluorescent single-walled carbon nanotubes via an oxygen-excluding surfactant organization, *Science* 323 (2009) 1319–1323, <http://dx.doi.org/10.1126/science.1166265>.
- [41] S. Ghosh, S.M. Bachilo, R.A. Simonette, K.M. Beckingham, R.B. Weisman, Oxygen doping modifies near-infrared band gaps in fluorescent single-walled carbon nanotubes, *Science* 330 (2010) 1656–1659, <http://dx.doi.org/10.1126/science.1196382>.